https://doi.org/10.5194/egusphere-2023-2822
Preprint. Discussion started: 4 December 2023

Climatic Controls on Metabolic Constraints in the Ocean

Precious Mongwe[1], Matthew Long[2], Takamitsu Ito[3], Curtis Deutsch[4], and Yeray Santana-Falcón[5]

[1]Southern Ocean Carbon Climate Observatory (SOCCO), CSIR, Cape Town, South Africa
[2]Oceanography Section, Climate and Global Dynamics Laboratory, National Center for Atmospheric Research, Boulder, CO, United States of America
[3]School of Earth and Atmospheric Sciences, Georgia Institute of Technology, Atlanta, Georgia United States of America
[4]Department of Geosciences, Princeton University, Princeton, NJ, United States of America
[5]CNRM, Université de Toulouse, Météo-France, CNRS, Toulouse, 31057, France
Corresponding Author: Precious Mongwe (pmongwe@csir.co.za)

Abstract

Observations and models indicate that climate warming is associated with the loss of dissolved oxygen from the ocean. Dissolved oxygen is a fundamental requirement for heterotrophic marine organisms (except marine mammals) and, since the basal metabolism of ectotherms increases with temperature, warming increases organisms' oxygen demand. Therefore, warming and deoxygenation pose a compound threat to marine ecosystems. In this study, we leverage an ecophysiological framework and compilation of empirical trait data quantifying the temperature sensitivity and oxygen requirements of metabolic rates for a range of marine species ("ecotypes"). Using the Community Earth System Model Large Ensemble, we investigate how natural climate variability and anthropogenic forcing impact the ability of marine environments to support aerobic metabolisms on interannual to multi-decadal timescales. Warming and deoxygenation projected over the next several decades will yield a reduction in the volume of viable ocean habitat. We find that fluctuations in temperature and oxygen associated with natural variability are distinct from those associated with anthropogenic forcing in the upper ocean. Further, the joint temperature-oxygen anthropogenic signals emerges sooner than independently from natural variability. Our results demonstrate that anthropogenic perturbations underway in the ocean will strongly exceed those associated with the natural system; in many regions, organisms will be pushed closer to or beyond their physiological limits, leaving the ecosystem more vulnerable to extreme temperature-oxygen events.

https://doi.org/10.5194/egusphere-2023-2822
Preprint. Discussion started: 4 December 2023

1. Introduction

Dissolved oxygen (O_2) is a fundamental metabolic requirement for heterotrophic marine organisms, excluding marine mammals (Portner, 2002; Keeling et al., 2010; Tiano et al., 2014). O_2 is declining due to warming, a tendency long predicted by models (Keeling et al., 2010; Long et al., 2016; Oschlies et al., 2018) and recently found evident at the global scale in compilations of in situ observations (Schmidtko et al., 2017; Ito et al., 2017). Deoxygenation is driven by the direct effect of reduced oxygen solubility with warming compounded by buoyancy-induced stratification in the upper ocean, which weakens the ventilation-mediated supply of fresh oxygen to the ocean interior. While the full ecological impacts of ocean deoxygenation remain uncertain, it is clear that the physiological impacts of oxygen loss on marine organisms can be considered explicitly in the context of warming: basal metabolic rates for ectothermic organisms depend on ambient temperature and increase with warming (Gillooly et al., 2001); thus, higher temperatures impose additional demand for oxygen to sustain aerobic respiration (Deutsch et al., 2015). Consequently, as the ocean warms, even present-day oxygen distributions may be insufficient to meet the oxygen demands of organisms living near key physiological thresholds (Deutsch et al., 2022).

While model projections clearly demonstrate that warming and deoxygenation are consequences of human-driven climate change, it is important to recognize that natural climate variability also produces important fluctuations in these quantities. Indeed, evidence suggests that natural variability contributes to hypoxic events, such as those observed in the California Current, where fish and benthic-organism mortality has been associated with low-O_2 waters impinging on the continental shelf (Pozo Buil and Di Lorenzo, 2017; Howard et al., 2020). A clear understanding of how natural climate variability drives fluctuations in metabolic state and the associated implications for organisms is a critical context in which to view long-term climate warming. Given that the natural system is highly dynamic, climate change signals are often masked by decadal-scale variability (Ito and Deutsch, 2010). While numerous authors have considered detection and attribution of climate change for physical and biogeochemical variables (Rodgers et al., 2015; Long et al., 2016; Schlunegger et al., 2019), comparatively little attention has been devoted to explicitly characterizing the relative influence of natural and anthropogenic drivers of changes in the ocean's capacity to support aerobic life. In this study, we approach this challenge

https://doi.org/10.5194/egusphere-2023-2822
Preprint. Discussion started: 4 December 2023

by leveraging the concept of the Metabolic Index (Φ) introduced by Deutsch et al. (2015). Φ is based on the notion that aerobic organisms can persist only where the ambient oxygen partial pressure (pO_2) is sufficient to meet the requirements of sustaining respiration. Φ incorporates an explicit representation of the dependence of metabolic oxygen demand on temperature, thus providing a framework to consider how joint oxygen and temperature variability constrain viable habitat in the ocean.

Many ocean organisms may already be under threat from deoxygenation (Hoegh-Guldberg and Bruno, 2010; Breitburg et al., 2018); however, ongoing climate-driven loss of oxygen raises important questions about the future of marine ecosystems: How will anthropogenic changes in dissolved oxygen and temperature impact the capacity of ocean habitats to support aerobic metabolism? What is the spatial and temporal distribution of changes in the ocean's metabolic state associated with climate variability? At what point can anthropogenic change in the ocean's metabolic state be distinguished from natural variability? This study addresses these questions using a combination of metabolic theory, a dataset set quantifying key physiological parameters for a collection of marine species adapted to specific environments ("ecotypes"), and the oxygen and temperature distributions simulated in the Community Earth System Model, version 1 Large Ensemble (CESM1-LE), which includes 34 members simulating ocean biogeochemistry under climate variability and change from 1920–2100 forced using historical data and the Representative Concentration Pathway Scenario 8.5 (RCP85) (Kay et al., 2015; Long et al., 2016).

This paper is organized as follows. Section 2 presents a brief overview of the relevant metabolic theory, the associated empirical datasets, and describes our approach to analysis. In Section 3 we present results quantifying the joint temperature-oxygen variability simulated in the CESM1-LE, evaluating the spatiotemporal structure of variability in marine ecotype habitat, including long-term trends based on the RCP8.5 scenario and time of emergence (ToE). The main outcomes of the results are synthesized in Section 4 and summarized in Section 5.

2. Datasets and methods

https://doi.org/10.5194/egusphere-2023-2822
Preprint. Discussion started: 4 December 2023

2.1 Metabolic index

Empirical studies measuring thermal tolerance and oxygen requirements in the laboratory on an array of marine organisms have enabled an assessment of lethal thresholds (Vaquer-Sunyer and Duarte, 2008; Rosewarne et al., 2016). These data coupled with recent advances in a theoretical framework enable both explanatory and predictive power in the context of a dynamic environment (Deutsch et al., 2015; Penn et al., 2018; Howard et al., 2020). The fundamental insights here are that basal metabolic rates for ectothermic marine organisms depend on ambient temperature and generally increase with warming (Gillooly et al., 2001). Increasing basal metabolic rates impose additional demand for oxygen. Organisms use oxygen dissolved in seawater and acquisition tends to be limited by diffusive processes; thus, oxygen supply is related to the ambient pO_2. The ratio of oxygen supply to temperature-dependent demand provides a critical indicator of the capacity for an organism to meet its metabolic requirements. Deutsch et al. (2015) formalized these concepts into a quantity termed the "Metabolic Index (Φ)", which is defined as the ratio of oxygen supply to an organism's resting metabolic demand. Oxygen supply is parameterized according to a biomass-dependent scaling of pO_2, capturing variation in the efficiency with which organisms acquire and utilize O_2. This can be expressed as $S = \alpha_s B^{\sigma} pO_2$, where α_S is a mass-normalized coefficient expressing the rate of gas transfer between an organism and its environment and B^{δ} is the scaling of supply with biomass, B (Piiper et al., 1971). Resting metabolic demand can be expressed using the Arrhenius equation as

$$D = \alpha_D B^{\delta} exp\{\frac{-E_d}{K_B}\left[\frac{1}{T} - \frac{1}{T_{ref}}\right]\},$$

where α_D is a species-specific basal metabolic rate, B^{δ} is the scaling of this rate with biomass, E_d (eV) is the temperature dependence of oxygen supply, T is temperature, T_{ref} is the reference temperature (15°C), and k_B is the Boltzmann constant (Gillooly et al., 2001). Gas transfer is kinematically slow at low temperatures, and hence organism viability can be limited by the energy to acquire oxygen at low temperatures, thus E_o varies with temperature. Here we account for this by adding the temperature dependence (dE_o/dT) to E_o in equations above ($E_o + \frac{dE_o}{dT}(T - T_{ref})$), using the mean value of $dE_o/dT = 0.022$ eV consistent with Deutsch et al. (2020). The Metabolic Index can thus be written as the ratio of S/D:

$$\Phi = A_o pO_2 exp\{\frac{-E_o}{K_B}\left[\frac{1}{T} - \frac{1}{T_{ref}}\right]\}, \quad (1)$$

https://doi.org/10.5194/egusphere-2023-2822
Preprint. Discussion started: 4 December 2023

where $A_o = \alpha_S/\alpha_D$ *(1/atm)* is the hypoxic tolerance, $E_o = E_d - E_s$ (E_s is the temperature dependence of oxygen supply) (Deutsch et al., 2015; Penn et al., 2018). The exponent, $\varepsilon = \sigma - \delta$, is the allometric scaling of the supply to demand ratio with biomass, is typically near zero. Therefore, in the analysis that follows, we presume unit biomass and thus neglect potential impacts of variations in biomass.

If Φ falls below a critical threshold value of 1, conditions are physiologically unsustainable: an organism cannot meet its basic resting metabolic oxygen requirements. Conversely, values of Φ above 1 enable organismal metabolic rates to increase by a factor of Φ above resting levels, permitting critical activities such as feeding, defence, growth, and reproduction. Thus, for a given environment and species, Φ provides an estimate of the ratio of maximum sustainable metabolic rate to the minimum rate necessary for basal metabolism. Deutsch et al. (2015) inferred the ratio of active to resting energetic demand by examining the biogeographic distribution of several species, finding that range boundaries coincide with values of Φ = 1.5–7. This threshold, termed critical rate (Φ_{crit}), represents the minimum metabolic index required for an organism to sustain an active metabolic state, which is a more meaningful ecological threshold than requirements for resting metabolism. Therefore, in this study, we define a quantity Φ', which is derived by dividing Φ by Φ_{crit}; equivalently, this yields an adjusted definition of the hypoxic tolerance trait, $A_c = A_o / \Phi_{crit}$, where A_c is termed the "ecological hypoxia tolerance" consistent with Howard et al. (2020). Where $\Phi' > 1$ (i.e., $\Phi > \Phi_{crit}$) an organism can sustain an active metabolic rate; where $\Phi' < 1$ (i.e., $\Phi < \Phi_{crit}$), O_2 is insufficient and an active metabolic state is not viable. Henceforth, our analysis uses Φ' to characterize ecotypes viability.

2.2 Physiological dataset

We make use of a dataset describing physiological parameters for a collection of 61 marine ecotypes spanning a range of ecological hypoxic tolerances (A_c) and temperature sensitivities (E_o) (Penn et al., 2018; Deutsch et al., 2020, Figure 1a). We illustrate how the physiological traits E_o and A_c constrain habitat viability in the context of distributions of pO_2 and temperature in the marine environment in Figure 1b, which shows the minimum pO_2 (i.e., pO_2 at Φ_{crit}) required to sustain an active metabolic state as a function of temperature for five combinations of E_o and A_c.

https://doi.org/10.5194/egusphere-2023-2822
Preprint. Discussion started: 4 December 2023

153 The five combinations are derived from sampling the probability distributions of E_o and A_c
154 (Figure 1a) at the 10th, 50th, and 90th percentile values (illustrated by colored stars in Figure 1a
155 and corresponding curves in Figure 1b). We assume that the trait distributions are independent,
156 which is a reasonably modest simplification; E_o is represented by a normal distribution and A_c by
157 a lognormal distribution function (Figure S1). The pO_2 at Φ_{crit} curves shown in Figure 1b
158 delineate regions of pO_2-temperature space that are habitable (above the curve) and
159 uninhabitable (below the curve). The reversing curvature of pO_2 at Φ_{crit} in Figure 1b at low
160 temperature captures the decrease of the organism's oxygen acquisition efficiency in cooler
161 conditions yielding cold intolerance.

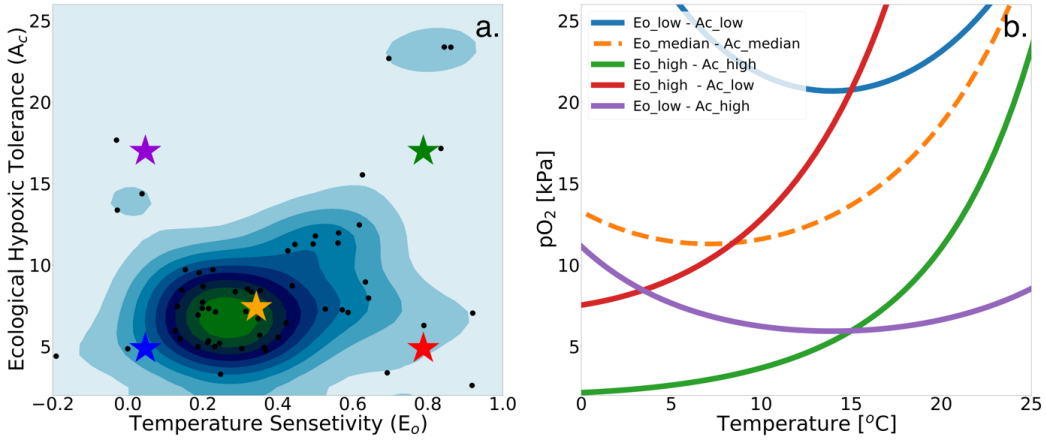

162
163 **Figure 1**. Physiological traits determining hypoxic tolerance. (a) Scatter plot of 61 marine ecotypes for which
164 empirically derived estimates of activation energy (E_o) and the ecological hypoxic tolerance (A_c) have been
165 determined (Penn et al., 2018). The color shows the density of occurrence for the 61 marine ecotypes in the A_c - E_o
166 trait space. (b) The minimum pO_2 required to sustain an active metabolic state (i.e., pO_2 at Φ_{crit}, Deutsch et al., 2020)
167 for five combinations of A_c and E_o corresponding to the stars in panel "a"; these are combinations of the 10th, 50th,
168 90th percentile values for each parameter.
169
170 To illustrate how the trait combinations of E_o and A_c exert control on the geographic distribution
171 of organisms in the marine environment (Deutsch et al., 2020), we use observations of pO_2 and T
172 along a zonal transect of the Pacific Ocean and plot Φ' for nine combinations of E_o and A_c
173 percentile values (Figure 2). The colorbar in Figures 2a-i show the metabolic index for an active
174 state (Φ'); regions with values above one are habitable (color), while regions with values below

https://doi.org/10.5194/egusphere-2023-2822
Preprint. Discussion started: 4 December 2023

one are uninhabitable (white) on the basis of metabolic constraints (other ecological considerations are not considered). The subplots in the upper portion of the figure are arranged according to the same trait axes shown in Figure 1a; E_o increases horizontally from left to right and A_c increases from the bottom to the top. For the trait combination in the bottom left (low E_o, low A_c; Figure 2g), metabolism is relatively insensitive to temperature, and tolerance for low pO_2 is poor. Thus, ecotypes with low E_o and low A_c are restricted to high latitude surface waters, where temperatures are cool, and pO_2 is abundant (Figure 2g). As E_o increases from left to right, metabolic rates become more sensitive to temperature. Then, habitat is gained at depth, where temperatures are cooler and higher temperature sensitivity confers an advantage (Figure 2g–i). From the bottom to the top, the increase in tolerance of low pO_2 conditions increases habitability in regions of low pO_2, enabling organisms to expand beyond high-latitude surface waters (Figure 2g-a). The biogeographic range for organisms with high A_c is modulated by E_o; as temperature sensitivity increases, ecotype viability at high latitudes is increased, but tropical surface waters become less viable (Figure 2 a-c). Henceforth, our analysis will utilize the metabolic index of the median ecotype (E_o = 0.34, A_c= 7.4; Figure 2e) for illustrative purposes; i.e., all metabolic index figures refer to this median ecotype unless otherwise stated.

https://doi.org/10.5194/egusphere-2023-2822
Preprint. Discussion started: 4 December 2023

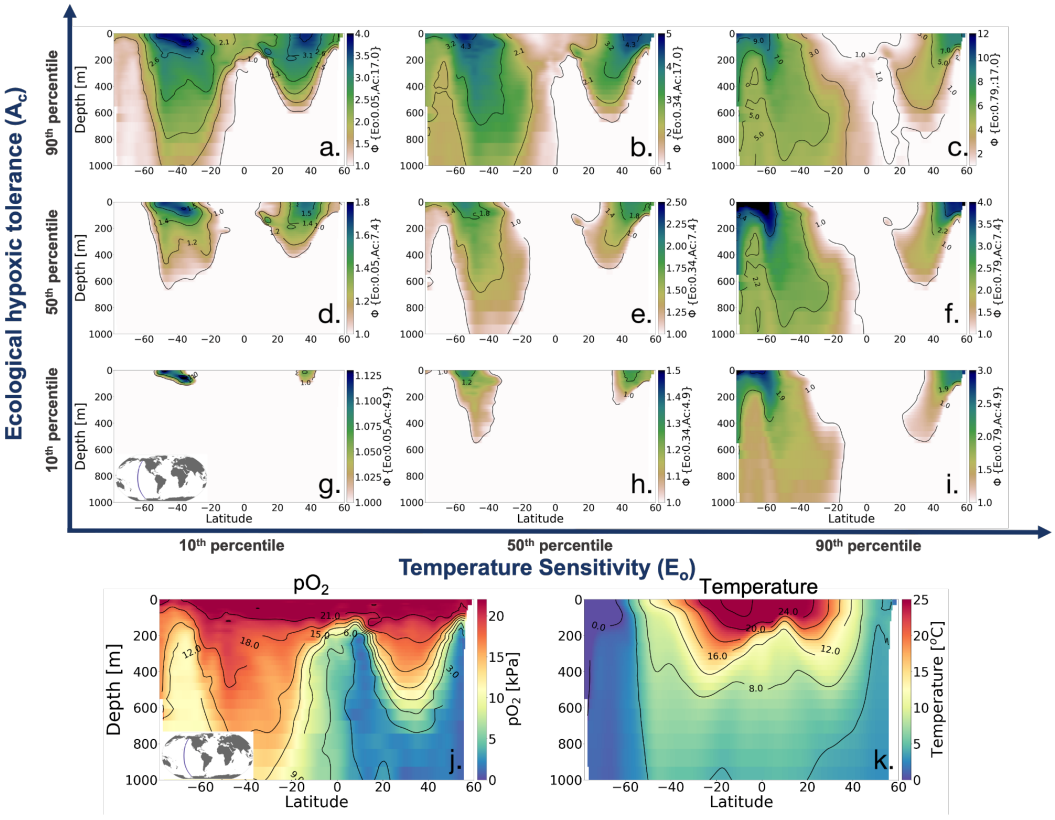

Figure 2. Annual mean metabolic index (Φ') for nine combinations of the ecological traits E_o (metabolic temperature sensitivity) and A_c (ecological hypoxic tolerance) along a transect in the Pacific Ocean based on a climatology from the World Ocean Atlas dataset (Garcia et al., 2014). The percentile values of each trait are: 10th (E_o = 0.04, A_c= 4.8), 50th (E_o = 0.34, A_c= 7.4), and 90th (E_o = 0.79, A_c= 17.0). The lower panels show pO_2 and temperature from the WOA dataset. Note that the colorbar range differs by panel and values where Φ' < 1 are omitted, thus the color shows only areas where an active metabolic state can be sustained.

2.3 Earth system model simulations

This study is based on the CESM1-LE, described in detail by Kay et al. (2015). The CESM1-LE included 34 ensemble members integrated from 1920–2100 under historical and RCP8.5 forcing. The ensemble was generated by adding round-off level (10^{-14} K) perturbations to the air temperature field at initialization in 1920; this small difference yields rapidly diverging model solutions due to the chaotic dynamics intrinsic to the climate system, thus developing ensemble spread representative of internal variability (Kay et al., 2015). Briefly, the CESM1-LE uses the

https://doi.org/10.5194/egusphere-2023-2822
Preprint. Discussion started: 4 December 2023

Community Earth System Model, version 1 (Hurrell et al., 2013), with a horizontal resolution of nominally 1° in all components. The ocean component is Parallel Ocean Program version 2, (Smith et al., 2010) with sea ice simulated by the Los Alamos Sea Ice Model version 4 (Hunke and Lipscomb, 2010). Ocean biogeochemistry was represented by the Biogeochemical Elemental Cycling (BEC) model (Moore et al., 2013; Lindsay et al., 2014).

Our analysis focuses on three depths: 50 m representing near-surface dynamics, the epipelagic zone at 200 m, and the mesopelagic zone at 500 m. pO_2 was calculated using the Garcia and Gordon. (1992) solubility formulation. For convenience, we use the period 1920–1965 to define a minimally-perturbed natural state, as this period is prior to the development of substantial anthropogenic trends in ocean oxygen and temperature (Long et al., 2016). We also examine distributions over the last three decades of the 21st century (2070–2099) to evaluate the projected climate-change signal under RCP8.5. We use the mean across all 34 ensemble members to quantify the deterministic, “forced” response of the climate system to anthropogenic influence (Deser et al., 2012). The ensemble spread is thus indicative of the amplitude of variations attributable to natural variability.

https://doi.org/10.5194/egusphere-2023-2822
Preprint. Discussion started: 4 December 2023

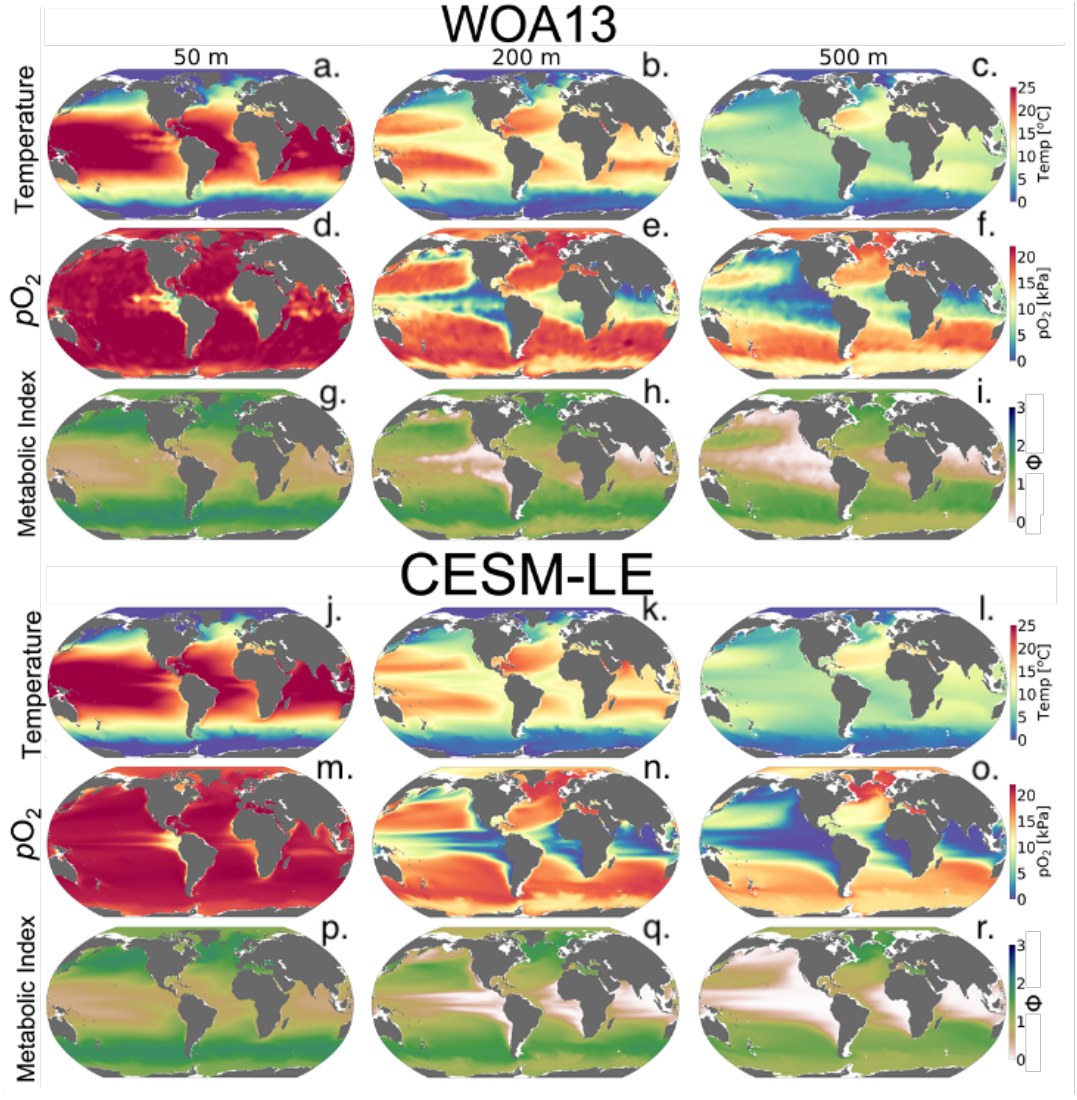

Figure 3. Mean-state comparison with observations. The climatological mean of (top rows) temperature (°C), (middle rows) pO_2 (kPa), and the (bottom rows) metabolic index for active metabolism (Φ') for the median ecotype (E_o = 0.34, A_c= 7.4); three depths are shown (left) 50 m, (center) 200 m, and (right) 500. Top panels show the WOA13 dataset and the bottom panels show CESM1-LE.

We compared the CESM1-LE (1920 - 1965) with the World Ocean Atlas, version 2013 (WOA2013) dataset (Garcia et al., 2014), an observationally-based, gridded climatology (Figure 3a-i). CESM1-LE generally provides a reasonable representation of pO_2 and temperature

https://doi.org/10.5194/egusphere-2023-2822
Preprint. Discussion started: 4 December 2023

distributions at the selected depths (Figure 3); however, there are important biases to acknowledge in the context of interpreting the results. Temperature magnitudes are generally well simulated in the CESM1-LE, showing a root mean square error (RMSE) < 1.3 °C, and pattern correlation coefficient (PCC) >0.98 in all three selected depths (50 m, 200 m, and 500) (Table 1). Temperature magnitudes are slightly underestimated at 50 m and 200 m (mean bias of < 0.3°C), and overestimated by 0.41 °C at 500 m. Note that since our comparison uses CESM1-LE data from 1920-1965, some discrepancy in temperature might be expected from the signal of climate warming present in the WOA observations. pO_2 is also reasonably well captured by the CESM1-LE (PCC <0.95), but magnitudes are slightly underestimated at depth, showing a mean bias of -1.63 kPa and -2.1 kPa at 200 m and 500 m with respect to WOA13 (Table 1). Regions of low pO_2 waters are too extensive in CESM1-LE (Figure 3n-o) and there is a slight degradation of skill with depth for pO_2 fields (Table 1). The underestimation of pO_2 leads to a slight underestimation of Φ' with respect to WOA13 (Figure 3 p-r); however, Φ' computed from the model fields demonstrates that the dominant spatial patterns are well captured by the CESM1-LE despite magnitudes that are slightly too low (i.e., Figure 1, c, l). These differences ultimately matter most near the hypoxic zones and at the boundaries of habitable zones like the OMZs.

https://doi.org/10.5194/egusphere-2023-2822
Preprint. Discussion started: 4 December 2023

Table 1. Summary statistics for the comparison of CESM1-LE with the World Ocean Atlas dataset (Garcia et al., 2014). The columns include the mean bias, pattern correlation coefficient (PCC), and root mean square error (RMSE) at 50 m, 200 m, and 500 m.

	Mean bias	**R**	**RMSE**
	Temperature [°C]		
50 m	-0.17	0.99	1.22
200 m	-0.25	0.99	1.22
500 m	0.10	0.98	0.63
	pO_2 [kPa]		
50 m	0.05	0.99	1.91
200 m	-1.17	0.96	5.96
500 m	-1.46	0.95	6.28
	Metabolic index		
50 m	0.01	0.99	0.02
200 m	-0.09	0.97	0.05
500 m	-0.15	0.96	0.08

https://doi.org/10.5194/egusphere-2023-2822
Preprint. Discussion started: 4 December 2023

2. Results

3.1 Joint temperature-pO_2 natural variability and forced trends

The spatial distribution of the number of viable ecotypes is shown in Figure 4 for the "unperturbed" climate (1920-1965). Our intention here is not to quantify the actual biogeographic range of organisms in the environment, but rather to illustrate the ocean's ability to support respiration by marine ectotherms given the metabolic capacities afforded within the trait space of extant organisms. High latitude environments do not impose strong aerobic constraints (cold intolerance notwithstanding), thus over much of the Southern Ocean, North Atlantic, and Arctic Ocean almost all 61 ecotypes can sustain respiration. The tropical oceans impose the strongest aerobic constraints, restricting the viability of ecotypes that do not have high-hypoxia tolerance (A_o). For example, less than 25 ecotypes are viable over much of the tropical surface ocean (Figure 4a); low concentrations of oxygen at depth impose even stronger constraints, and no ecotypes are viable in the core of OMZs (Figure 4b, c). The spatial patterns of the number of viable ecotypes is tightly controlled by temperature at the surface, since pO_2 is mostly near saturated levels; at depth, however, pO_2 is the dominant driver of geographic patterns in ecotype viability (Figures 2-4). Temperature generally decreases with depth, reducing the metabolic oxygen demand. However, since pO_2 also decreases with depth and displays greater lateral heterogeneity, pO_2 emerges as the dominant constraint of spatial structure in ecotype viability at depth.

The standard deviation of annual anomalies using all CESM1-LE ensemble members provides insight into the amplitude of natural variability (Figure. 5). Temperature and pO_2 show similar patterns of natural variability in the upper ocean, both showing particularly large variance in the western tropical Pacific and Indian Ocean (Figure 5 a, d). Spatial variation in the magnitude of temperature variability generally decreases with depth, but pO_2 displays even relatively larger variability at depth with respect to the surface in some regions (Figure 5 a–f). The joint pO_2-temperature variability manifests in variations of Φ' (Figure 5g-i). Natural variability in Φ' computed for the median ecotype shows spatial patterns similar to temperature in the upper-

https://doi.org/10.5194/egusphere-2023-2822
Preprint. Discussion started: 4 December 2023

surface ocean (50 m), but is more similar to pO_2 at depth. Thus, variations in Φ' tend to be temperature-dominated near the surface, but are more strongly controlled by pO_2 variability at depth. Φ' also shows the most extensive natural variability at 200 m consistent with the variability of pO_2. The number of viable species shows more dramatic fluctuations than variations in the median ecotype Φ'; variations in the number of viable ecotypes exceed 30% on annual timescales in the tropical upper ocean and near OMZ boundaries in the water column (Figure 4 c–d). This reflects the fact that interannual variability can preclude habitability for some regions of the A_c-E_o trait space, but these variations do not necessarily impact viability for the median ecotype (Figure 1). In the tropical surface ocean, high temperatures (>25ºC), and saturated surface (pO_2 >20 kPa) require high hypoxia tolerance (A_c), but permit a range of E_o values (Figure 1b, 2a-b). Ecotypes with larger temperature sensitivity (high E_o) are particularly responsive to variations in temperature.

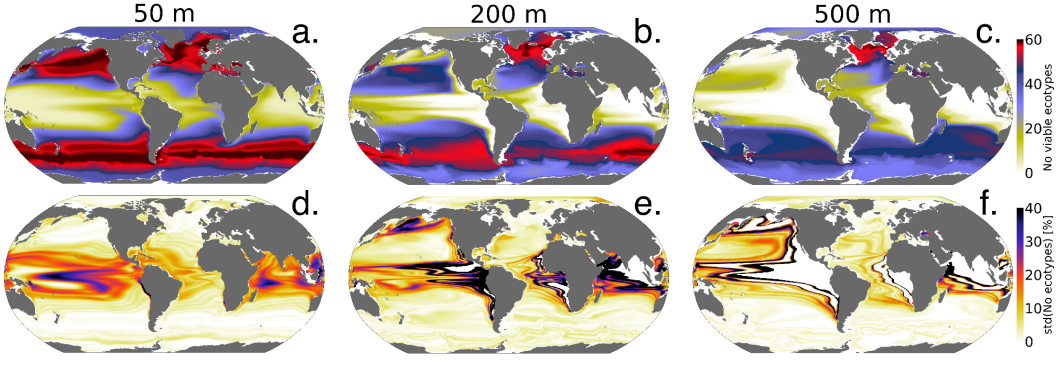

Figure 4. Metabolic constraints on trait-space viability. Top row: the number of ecotypes from the physiological trait database that are viable (total = 61) in the CESM1-LE over the period 1920–1965. Bottom row: the standard deviation (expressed as a percent of the mean) in the number of viable ecotypes, reflecting fluctuations driven by natural variability.

https://doi.org/10.5194/egusphere-2023-2822
Preprint. Discussion started: 4 December 2023

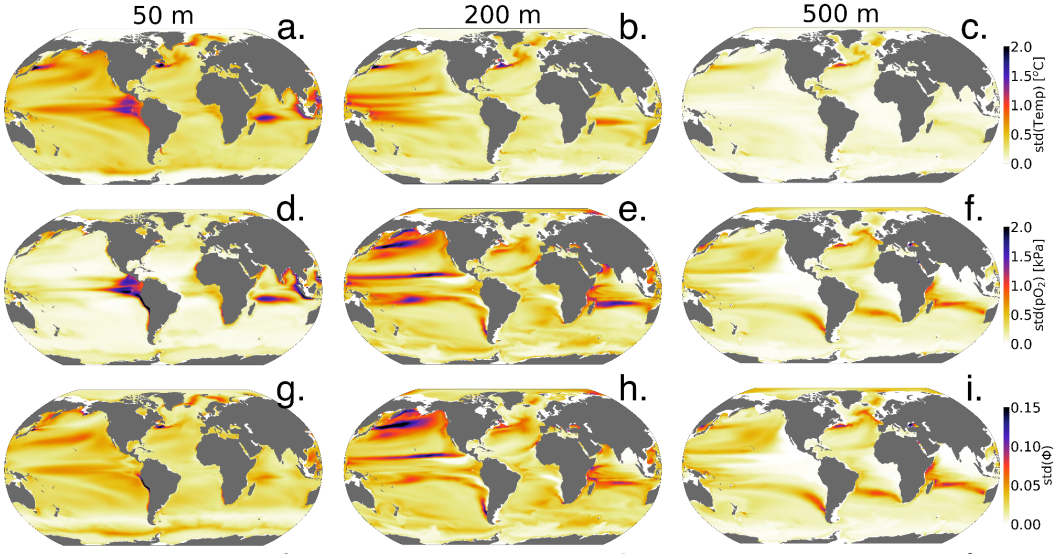

Figure 5. The amplitude of natural variability in the ocean's metabolic state. The panels show the standard deviation of annual-mean anomalies of all ensemble members over the period 1920–1965 for (top row) temperature (°C), (middle row) pO_2 (kPa), and (bottom row) the metabolic index (unitless) of the median ecotype (E_o = 0.34, A_c= 7.4).

CESM1-LE simulates nearly homogeneous warming between 1920–1965 and 2070–2099 in the surface ocean (50 m) under RCP8.5, with an exception of the so-called North Atlantic warming hole (Figure 6a). Both modelling and observational studies have linked the North Atlantic warming hole to the slowing of the Atlantic overturning circulation with climate change (Keil et al., 2020). The magnitude of ocean warming generally diminishes with depth except in the North Atlantic, where, despite reductions, the overturning circulation effectively propagates anthropogenic heat anomalies into the ocean interior. pO_2 shows heterogeneous changes between 1920–1965 and 2070–2099 (Figure 6 d-f). In the upper ocean, pO_2 changes are generally small (< 1 kPa) because the near-surface is kept close to saturation via photosynthetic oxygen production and air-sea equilibration. At depth, however, pO_2 shows long-term changes linked to accumulated effects of respiration and changes in circulation (Ito et al., 2017). At 200 m for example, the Pacific Ocean displays a basin-wide mean reduction in pO_2 of 2 kPa (~30%), while the Atlantic and Indian basins gain about >2 kPa (~ 10 - 35%) by the end of the century. The largest long-term pO_2 loss (>3 kPa) occurs in the North Pacific while the largest pO_2 gain (~2

https://doi.org/10.5194/egusphere-2023-2822
Preprint. Discussion started: 4 December 2023

kPa) occurs in the North Atlantic gyre and western Indian Ocean (Figure 6 e-f).

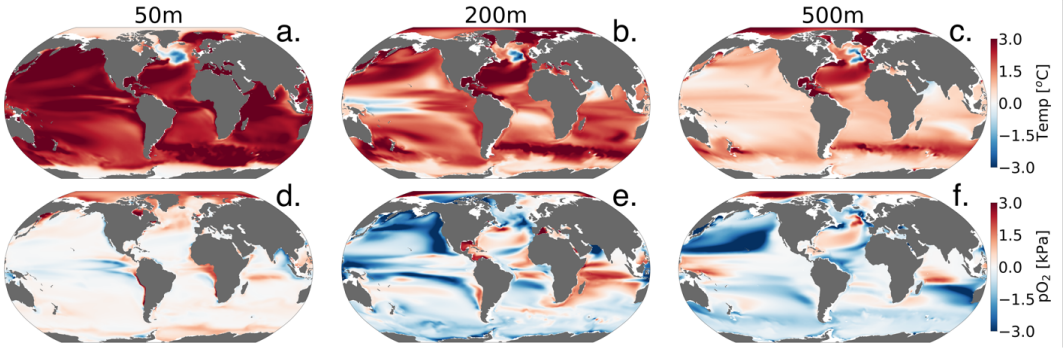

Figure 6. Net long-term change (2070–2099 minus 1920–1965) in the CESM1-LE ensemble means temperature (top) and (bottom) pO_2 at 50 m, 200 m, and 500 m.

Figure 7 shows the relationship between interannual variations in pO_2 versus temperature (pO_2-T) in the unperturbed climate (1920–1965; top row) and for the forced trend associated with 21st century climate change (2070–2099 minus 1920–1965; bottom row). The nature of the pO_2-T relationship is an important indicator of the impacts of variability on the metabolic state. Furthermore, the extent to which the forced trend is characterized by a pO_2-T relationship that is distinct from that associated with natural variability provides insight into the potential for advanced or delayed detection of signals in Φ relative to pO_2 or temperature alone. Given that metabolic rates for most organisms increase with temperature (positive E_o), a positive correlation between variations in temperature and pO_2 is generally indicative of compensating changes, wherein increased oxygen demand is at least partially offset by increased supply. Anticorrelation between temperature and pO_2, by contrast, will generally be associated with compounding impacts on the metabolic index, as a negative correlation indicates that reductions in pO_2 (i.e., oxygen supply) accompany warming (i.e., increased demand). The sign of the pO_2-T relationship in the natural climate varies regionally and with depth (Figure 7, top row). The surface ocean is generally characterized by a weak, positive pO_2-T relationship, which could manifest from, among other mechanisms, temperature-induced increases in photosynthetic oxygen production (Figure 7a). The natural pO_2-T relationship in the epipelagic (200 m) is characterized by strong positive correlations in the tropics and negative correlations at high latitudes (Figure 7b). A positive correlation between pO_2 and temperature at this depth could be induced by variability

https://doi.org/10.5194/egusphere-2023-2822
Preprint. Discussion started: 4 December 2023

associated with adiabatic vertical displacement of isopycnals, or "heave", which has the effect of translating background gradients in properties vertically in the water column. Upward movement of a deep isopycnal surface would yield a negative temperature anomaly and a negative pO_2 anomaly (positive correlation), as the deeper, colder waters have greater oxygen utilization signatures associated with longer ventilation age. Negative correlations between pO_2 and temperature could manifest from ventilation processes, where enhanced subduction of surface water yields anomalously cold water masses that are enriched in oxygen. The sign of these epipelagic pO_2-T correlations shows some similarity to those associated with the externally forced climate (Figure 6e), but the latter is characterized by a greater prevalence of anticorrelation, most notably in the North Pacific ocean. At 500 m depth, the relationship between temperature and pO_2 in the natural climate is almost a mirror image of the epipelagic (Figure 7c); the tropics generally display negative correlations, while polar regions show positive correlations (Figure 7 e). The pO_2-T relationship in the forced trend at 500 m is dominated by broad regions of deeply negative correlations, with the most pronounced effect again in the North Pacific. The negative relationship is consistent with a ventilation signal, as buoyancy-induced stratification from warming curtails the introduction of new oxygen into the ocean interior. The predominantly negative pO_2-T relationship associated with the forced trend is indicative of the compounding effects of climate change on metabolic state, increasing metabolic demand while simultaneously reducing oxygen supply.

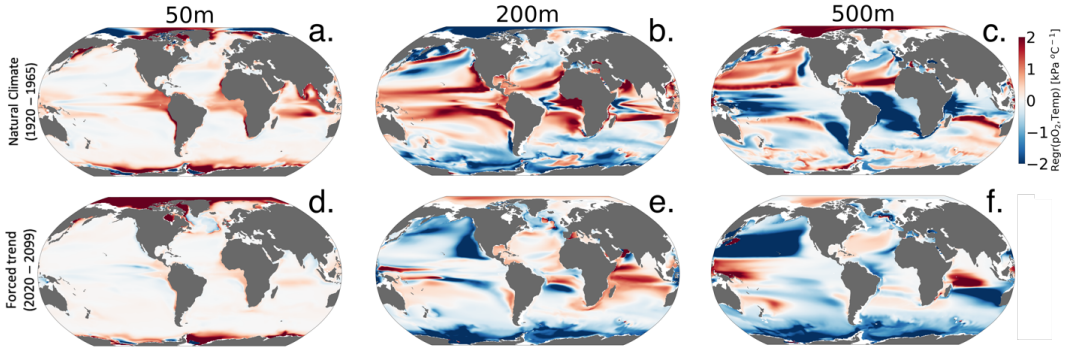

Figure 7. Regression of annual means pO_2 versus temperature (kPa $^{o}C^{-1}$) for (top row) interannual variability and (bottom row) the forced trend (difference between 2020–2099 and 1920–1965). The columns show the regressions computed at different depths, 50 m, 200 m, and 500 m, respectively.

https://doi.org/10.5194/egusphere-2023-2822
Preprint. Discussion started: 4 December 2023

3.2 Long-term habitat changes

Figure 8 shows the climate-driven changes in Φ' for the median ecotype, as well as the impacts of climate change on the number of viable ecotypes. Notably, while pO_2 in the near-surface ocean is relatively insensitive to climate change (Figure 6d), there are reductions in Φ' in the tropics (Figure 9d), owing to the direct impacts of warming. These changes are associated with deep reductions in the number of viable ecotypes in the tropics (Figure 8a). There are modest increases in Φ' and ecotype viability at high-latitudes; metabolic state in these regions is affected by cold intolerance, thus warming broadens the viable region of trait space. Additionally, reductions in sea ice cause an increase in pO_2, as gas exchange becomes more effective at restoring equilibrium oxygen concentrations. The number of viable ecotypes shows more intense patterns than those in the median ecotype Φ' in the upper ocean (Figure 8). This is partly because ecotypes predicted to lose viability in the tropical regions (~ 50%) are at the extremes of the A_c-E_o distribution (Figure 1) and not captured by the median ecotype Φ'. Nevertheless, outside the tropical regions, the median ecotype gives a good indication of the anthropogenic impact to marine ectotherms. The projected habitat loss in the epipelagic-pelagic North Pacific (> 50%) and habitat gain in the epipelagic-pelagic Southern Indian Ocean (~40%) and pelagic western tropical regions (~40%) are consistent with a decrease in the median ecotype Φ'. Note that the most pronounced effects on habitat are associated with regions where climate change drives a strongly negative pO_2-temperature relationship (Figure 7).

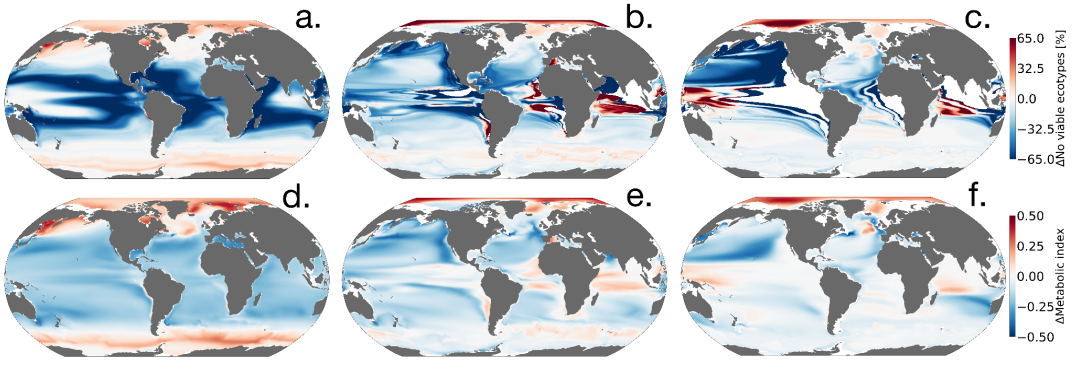

Figure 8. Net change in the number of habitable ecotypes in percentage (top row). Net metabolic index change (2070 - 2099 vs. 1920 - 1965) for the median ecotype [E_o = 0.34, A_c= 7.4] (bottom row). At 50m (first column), 200m (second column) and 500m (third column).

https://doi.org/10.5194/egusphere-2023-2822
Preprint. Discussion started: 4 December 2023

3.3 Time of Emergence

In this section, we examine the "time of emergence" (ToE, Hawkins and Sutton, 2012), the point when forced changes in pO_2, temperature and Φ' can be distinguished from the background natural variability. We define ToE as the time when the magnitude of change in the ensemble mean of a particular variable exceeds two standard deviations of the natural climate (1920 - 1965). This is illustrated in Figure 9 for a single grid point in the North Pacific at 200 m. At this location, the forced trend in temperature shows a monotonic increase, while pO_2 shows a monotonic decrease; as a result, Φ' for the median ecotype and the number of viable ecotypes decrease over time. The anti-correlation between pO_2 and temperature exacerbates trends in Φ', and hence the forced trend of the median ecotype Φ' emerges from natural noise earlier than either pO_2 or temperature do alone (Figure 10a-c). Note that although the ToE of ecotype viability change is directly derived from changes in Φ', it is binary counted; changes in ecotype viability are counted in whole numbers and this creates a step-function temporal-spatial variation (Figure 9d). Consequently, this step-function-like feature of ecotype viability creates discontinuities even in spatial patterns of ToE (Figure 10 j-l) as also shown in the natural variance in Figure 4 d-f.

https://doi.org/10.5194/egusphere-2023-2822
Preprint. Discussion started: 4 December 2023

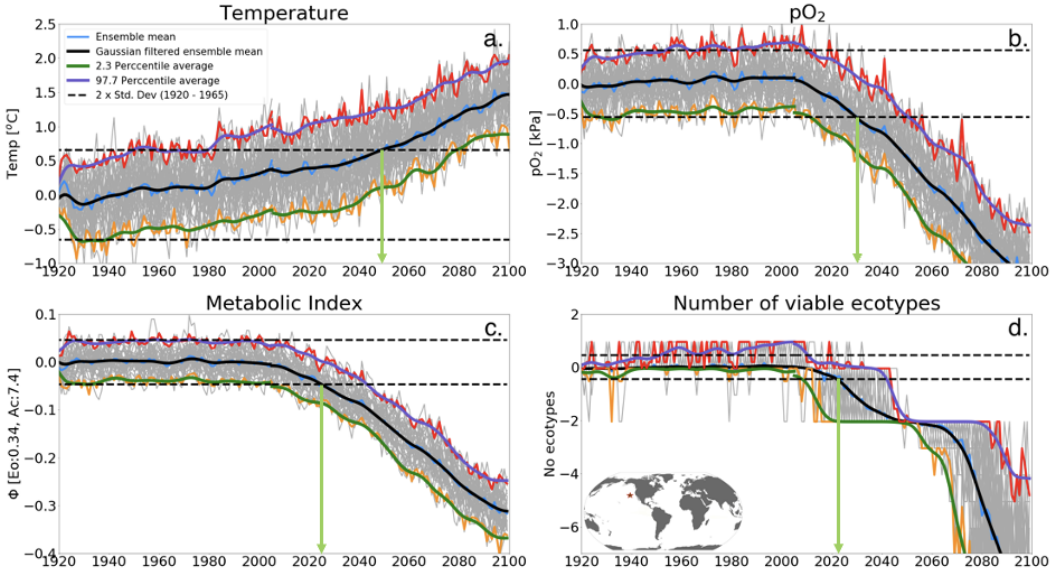

Figure 9.. Time of emergence (ToE) of the climate forcing signal for (a) temperature, (b) pO_2 (c) the metabolic index of the median ecotype [E_o = 0.34, A_c= 7.4], and (d) the number of viable ecotypes for a single model grid in the North Pacific at 200 m. ToE (green arrows) is defined as the time when the forced trend signal (ensemble member time series) is above two standard deviations (black dotted line) of all ensemble members for the period 1920 - 1965.

https://doi.org/10.5194/egusphere-2023-2822
Preprint. Discussion started: 4 December 2023

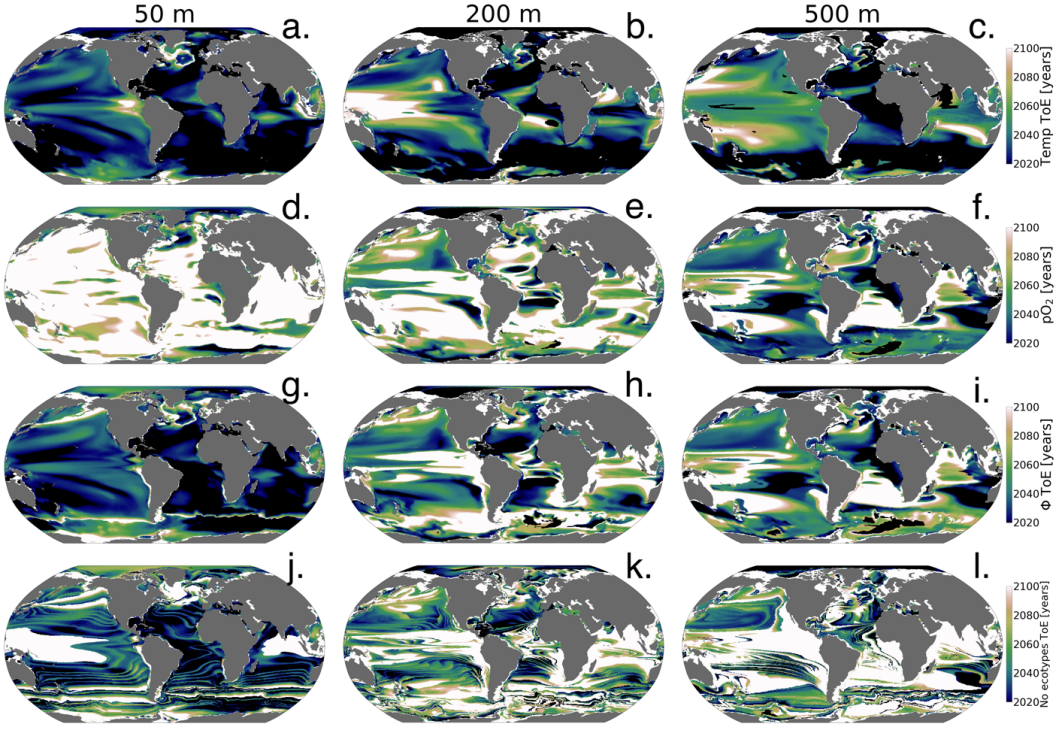

Figure 10. Time of emergence (ToE) of the climate forcing signal for temperature, pO_2, phi, and the number of viable ecotypes. ToE is defined as the time when the forced trend signal (ensemble member time series) is above two standard deviations of all ensemble members for the period 1920 - 1965.

The ToE of pO_2 and temperature are inverted with depth; temperature emerges earliest in the upper ocean while pO_2 emerges earlier at depth and later or shows no emergence in the upper ocean (Figure 10 a-f). This feature is consistent with larger upper ocean temperatures long-term changes and greater pO_2 changes at depth. Near-surface ocean temperature has mostly already emerged by 2020 and is predicted to have almost completely emerged by the late 2060s under RCP85 (Figure 10 a-c). The early emergence of temperature from natural noise also persists for regions of relatively low natural variance at depth, e.g., the Southern Ocean and Atlantic Basin Gyres. Regions of the largest natural variability (see Figure 5) like the subtropical-subpolar Pacific however do not emerge until close to the end of the century. For pO_2, anthropogenic changes in the upper ocean generally do not emerge from natural noise before the end of the century except for the Arctic Ocean and Eastern Antarctic. In the Arctic Ocean and Eastern

https://doi.org/10.5194/egusphere-2023-2822
Preprint. Discussion started: 4 December 2023

Antarctic pO_2 gain is related to sea-melt emergence by the mid-2050s (Figure 10a). The median ecotype Φ' ToE shows spatial patterns that are coherent with temperature ToE in the upper ocean with exception of polar regions. In contrast, they are consistent with pO_2 ToE patterns at depth; this is consistent with net long-term Φ' changes in Figure 9d. The emergence of the anthropogenic signal in ecotype viability closely resembles the median ecotype Φ' spatial patterns but showing non-harmonious spatial patterns due to the step-function-like counting feature of viability changes. It shows that the predicted ~ 50% ecotype viability loss in the tropics (Figure 6a) may already be distinguishable from natural variability by the mid-2030s. In the North Pacific, the predicted > 50% ecotype viability loss in the epipelagic-pelagic regions is predicted to start emerging in the 2040s at 500 m and 2080s at 200 m (Figure 10 k-l).

4. Discussion

The human-induced rapid warming of the planet has been shown to drive ocean deoxygenation (Ito et al., 2017; Schmidtko et al., 2017; Long et al., 2016). Higher metabolic oxygen demand at higher temperatures (Gillooly et al., 2001; Deutsch et al., 2015, 2022) raises concerns about the ability of marine ectotherms to support aerobic respiration in the future. This study set out to characterize the anticipated climate change signal in the ocean's metabolic state in the context of natural variability using the metabolic theory as a basis to examine the capacity of the environment to support ectothermic marine heterotrophs.

The spatial variation in pO_2 and temperature in the unperturbed natural climate state set biogeographic boundaries based on ectotherms' physiological performance. The resilience of these ectotherms' biogeographic structure to natural variability and long-term climate warming is perturbed by the joint pO_2-temperature changes, effectively measured by the metabolic index (Φ'). An increase in the capacity of the organisms to support aerobic respiration increases Φ'; for example by ocean cooling or increase in oxygen supply contrary, warming and decrease in oxygen supply decrease Φ'. There are exceptions in extremely low-temperature environments, where aerobic respiration is also limited by kinematic gas transfer into the organism in addition to environmental oxygen supply. Relative changes in pO_2 and temperature in the natural

https://doi.org/10.5194/egusphere-2023-2822
Preprint. Discussion started: 4 December 2023

variability and forced trend, therefore, regulate ectotherms' resilience to environmental changes. Under the RCP85 climate scenario, the ocean generally warms homogeneously but concurrent pO_2 changes are heterogeneous and vary with depth. Thus, the characteristics of these pO_2-temperature forced trend changes determine when the climate change impact on marine ectotherms can be distinguishable from natural variability.

In the surface ocean, pO_2 is generally abundant and relatively uniform, and thus spatial temperature variations have a dominant constraint on the spatial variations of organismic metabolic state. The warmest parts of the surface ocean, the tropical oceans, can only support about 10-20 (~ 30%) of the 61 ecotypes while cooler regions in extratropics have nearly 100% viability. Moreover, since warming anomalies propagate from the surface, the surface tropical oceans also show the largest natural variance in temperature and ecotype viability in the surface ocean. This is because extremely warm temperatures in the surface tropics (>25°C) are mainly suited for organisms with high-temperature sensitivity (E_o), which are relatively fewer, and mostly close to their physiological limits (Storch et al., 2014). Large natural variability in these warmest parts of the tropical surface ocean precludes the forced trend signal from emerging from the natural variability in the ecotype viability by end of the century although the ocean warms the largest in the surface. Nevertheless, the large warming trends in the surface ocean generally emerge relatively early (the 2020s) from natural variability in both temperature and ecotype viability in most regions. Minimal changes in surface pO_2 in the forced trend affirm that surface ocean marine ectotherms are mainly perturbed by temperature in the context of anthropogenic changes. In polar regions, warming has a counterintuitive effect on marine ectotherms with respect to most parts of the surface ocean. There, warming helps organisms escape extreme cold intolerances by enhancing membrane kinematic gas transfer which enhances Φ' and thus ecotype richness in the future.

In the epipelagic and pelagic regions (200 m and 500 m), the temperature forced trend and natural variability are smaller compared to the surface ocean, while concurrent pO_2 changes are larger than the surface ocean. Thus, pO_2 and temperature play a more intricate role in perturbating marine ectotherm habitats in the context of anthropogenic warming with respect to the surface ocean, where temperature plays a dominant role. At depth, contrasting the regression

https://doi.org/10.5194/egusphere-2023-2822
Preprint. Discussion started: 4 December 2023

between pO_2 and temperature in the natural climate, and forced trends provides an instructive framework to analyzing ectotherms' long-term changes. Regions showing distinct correlations between temperature and pO_2 in the forced trends relative to the natural variability show a weakening metabolic resilience; loss of habitat and emerging relatively early from natural variability. For example, in the pelagic - epipelagic North Pacific, temperature-pO_2 regressions switched from a positive correlation in the unperturbed climate to a strong negative correlation in the forced trend. Consequently, the pelagic-epipelagic North Pacific is projected to lose nearly half of the present climate ecotype viability by the end of the century. This loss of pelagic - epipelagic North Pacific habitat is projected to emerge earliest at 500 m (the 2030s) where anthropogenic pO_2 losses are larger than at 200 m. On the other hand, in the Arctic Ocean and some parts of the Southern Ocean, concomitant pO_2-temperature correlations in the forced trends result in the preservation of the marine habitat and even slight enhancements.

5. Conclusions

The joint temperature-oxygen metabolic framework in this study provides additional insight into the impact of climate change on marine ecosystems in comparison to the independent oxygen or temperature analysis. We here showed that while warming is the leading order driving mechanism of climate change, the direct effect of warming on marine ecosystems is mostly in the upper ocean. Climate change-related oxygen loss is a major driver of marine ecosystem stress in addition to warming at depth. Incorporating organismal physiological sensitivity to oxygen-temperature changes in the metabolic framework provides insight into how climate impacts the biogeographic structure of marine habitat. We find that underway forced trends perturbations in pO_2 and temperature will strongly exceed those associated with the natural system in many parts of the upper ocean, mostly pushing organisms in these environments closer to or beyond their physiological limits. Climate warming is expected to drive significant marine habitat loss in the surface tropical oceans and epipelagic - pelagic North Pacific Basin, while gaining marginal habitat viability in the surface Arctic Ocean and some parts of the Ocean Southern.

6. Competing interests

https://doi.org/10.5194/egusphere-2023-2822
Preprint. Discussion started: 4 December 2023

The contact author has declared that none of the authors has any competing interests

7. Acknowledgments

PM, ML, CD and TI were funded by the National Science Foundation (NSF) grant agreement No. 1737158. PM and YSF were also funded by the European Union's Horizon 2020 research and innovation programme under grant agreement No. 820989 (COMFORT).). We also would like to acknowledge the data access and computing support provided by the NCAR Cheyenne HPC.

8. Author contribution

PM and ML designed the study approach. PM developed the model code and analysis with feedback from ML, CD and TI. PM prepared the manuscript with contributions from all co-authors.

9. Data access

The CESM1 large ensemble data used in this study can be accessed in this location: https://www.cesm.ucar.edu/community-projects/lens/data-sets

10. References

Breitburg, D., Levin, L. A., Oschlies, A., Grégoire, M., Chavez, F. P., Conley, D. J., Garçon, V., Gilbert, D., Gutiérrez, D., Isensee, K., Jacinto, G. S., Limburg, K. E., Montes, I., Naqvi, S. W. A., Pitcher, G. C., Rabalais, N. N., Roman, M. R., Rose, K. A., Seibel, B. A., Telszewski, M., Yasuhara, M., and Zhang, J.: Declining oxygen in the global ocean and coastal waters, https://doi.org/10.1126/science.aam7240, 5 January 2018.

Deser, C., Phillips, A., Bourdette, V., and Teng, H.: Uncertainty in climate change projections: The role of internal variability, Clim Dyn, 38, 527–546, https://doi.org/10.1007/s00382-010-0977-x, 2012.

https://doi.org/10.5194/egusphere-2023-2822
Preprint. Discussion started: 4 December 2023

561 Deutsch, C., Ferrel, A., Seibel, B., Pörtner, H. O., and Huey, R. B.: Climate change tightens a
562 metabolic constraint on marine habitats, Science (1979), 348, 1132–1135,
563 https://doi.org/10.1126/science.aaa1605, 2015.
564
565 Deutsch, C., Penn, J. L., and Seibel, B.: Metabolic trait diversity shapes marine biogeography,
566 Nature, 585, 557–562, https://doi.org/10.1038/s41586-020-2721-y, 2020.
567
568 Deutsch, C., Penn, J. L., Verberk, W. C. E. P., Inomura, K., Endress, M.-G., and Payne, J. L.:
569 Impact of warming on aquatic body sizes explained by metabolic scaling from microbes to
570 macrofauna, https://doi.org/10.1073/pnas, 2022.
571
572 Garcia, H. E. and Gordon, L. I.: Oxygen solubility in seawater: Better fitting equations,
573 https://doi.org/10.4319/lo.1992.37.6.1307, 1992.
574
575 Garcia, H. E. , Boyer, T. P. , Locarnini, R. A. , Antonov, J. I. , Mishonov, A. V. , Baranova, O.
576 K. , Melissa, M. Z. , Reagan, J. R. , and Johnson, D. R. ,: WORLD OCEAN ATLAS 2013
577 Volume 3: Dissolved Oxygen, Apparent Oxygen Utilization, and Oxygen Saturation, 75,
578 https://doi.org/10.7289/V5XG9P2W, 2014.
579
580 Gillooly, J., Brown, J., West, G., Savage, V., Charnov, E., Gillooly, J. F., Brown, J. H., West, G.
581 B., Savage, V. M., and Charnov, E. L.: Effects of size and temperature on metabolic rate
582 Recommended Citation, 2001.
583
584 Hawkins, E. and Sutton, R.: Time of emergence of climate signals, Geophys Res Lett, 39,
585 https://doi.org/10.1029/2011GL050087, 2012.
586
587 Hoegh-Guldberg, O. and Bruno, J. F.: The Impact of Climate Change on the World's Marine
588 Ecosystems, New Series, 328, 1523–1528, https://doi.org/10.1126/science.ll85779, 2010.
589 Howard, E. M., Penn, J. L., Frenzel, H., Seibel, B. A., Bianchi, D., Renault, L., Kessouri, F.,
590 Sutula, M. A., Mcwilliams, J. C., and Deutsch, C.: Climate-driven aerobic habitat loss in the
591 California Current System, 2020.
592
593 Hunke, E. C. and Lipscomb, W. H.: CICE: the Los Alamos Sea Ice Model Documentation and
594 Software User's Manual Version 4.1 LA-CC-06-012, 2010.
595
596 Hurrell, J. W., Holland, M. M., Gent, P. R., Ghan, S., Kay, J. E., Kushner, P. J., Lamarque, J. F.,
597 Large, W. G., Lawrence, D., Lindsay, K., Lipscomb, W. H., Long, M. C., Mahowald, N., Marsh,
598 D. R., Neale, R. B., Rasch, P., Vavrus, S., Vertenstein, M., Bader, D., Collins, W. D., Hack, J. J.,
599 Kiehl, J., and Marshall, S.: The community earth system model: A framework for collaborative

https://doi.org/10.5194/egusphere-2023-2822
Preprint. Discussion started: 4 December 2023

research, Bull Am Meteorol Soc, 94, 1339–1360, https://doi.org/10.1175/BAMS-D-12-00121.1, 2013.

Ito, T. and Deutsch, C.: A conceptual model for the temporal spectrum of oceanic oxygen variability, Geophys Res Lett, 37, https://doi.org/10.1029/2009GL041595, 2010.

Ito, T., Minobe, S., Long, M. C., and Deutsch, C.: Upper ocean O2 trends: 1958–2015, Geophys Res Lett, 44, 4214–4223, https://doi.org/10.1002/2017GL073613, 2017.

Kay, J. E., Deser, C., Phillips, A., Mai, A., Hannay, C., Strand, G., Arblaster, J. M., Bates, S. C., Danabasoglu, G., Edwards, J., Holland, M., Kushner, P., Lamarque, J. F., Lawrence, D., Lindsay, K., Middleton, A., Munoz, E., Neale, R., Oleson, K., Polvani, L., and Vertenstein, M.: The community earth system model (CESM) large ensemble project : A community resource for studying climate change in the presence of internal climate variability, Bull Am Meteorol Soc, 96, 1333–1349, https://doi.org/10.1175/BAMS-D-13-00255.1, 2015.

Keeling, R. F., Körtzinger, A., and Gruber, N.: Ocean deoxygenation in a warming world, Ann Rev Mar Sci, 2, 199–229, https://doi.org/10.1146/annurev.marine.010908.163855, 2010.
Keil, P., Mauritsen, T., Jungclaus, J., Hedemann, C., Olonscheck, D., and Ghosh, R.: Multiple drivers of the North Atlantic warming hole, Nat Clim Chang, 10, 667–671, https://doi.org/10.1038/s41558-020-0819-8, 2020.

Lindsay, K., Bonan, G. B., Doney, S. C., Hoffman, F. M., Lawrence, D. M., Long, M. C., Mahowald, N. M., Moore, J. K., Randerson, J. T., and Thornton, P. E.: Preindustrial-control and twentieth-century carbon cycle experiments with the Earth system model CESM1(BGC), J Clim, 27, 8981–9005, https://doi.org/10.1175/JCLI-D-12-00565.1, 2014.

Long, M. C., Deutsch, C., and Ito, T.: Finding forced trends in oceanic oxygen, Global Biogeochem Cycles, 30, 381–397, https://doi.org/10.1002/2015GB005310, 2016.

Moore, J. K., Lindsay, K., Doney, S. C., Long, M. C., and Misumi, K.: Marine ecosystem dynamics and biogeochemical cycling in the community earth system model [CESM1(BGC)]: Comparison of the 1990s with the 2090s under the RCP4.5 and RCP8.5 scenarios, J Clim, 26, 9291–9312, https://doi.org/10.1175/JCLI-D-12-00566.1, 2013.

Oschlies, A., Brandt, P., Stramma, L., and Schmidtko, S.: Drivers and mechanisms of ocean deoxygenation, https://doi.org/10.1038/s41561-018-0152-2, 1 July 2018.

https://doi.org/10.5194/egusphere-2023-2822
Preprint. Discussion started: 4 December 2023

638 Penn, J. L., Deutsch, C., Payne, J. L., and Sperling, E. A.: Temperature-dependent hypoxia
639 explains biogeography and severity of end-Permian marine mass extinction, Science (1979), 362,
640 https://doi.org/10.1126/science.aat1327, 2018.
641
642 Piiper, J., Dejours', P., Haab, P., and Rahn, H.: CONCEPTS AND BASIC QUANTITIES IN
643 GAS EXCHANGE PHYSIOLOGY, Respiration Physiology, 292–304 pp., 1971.
644 Portner, H. O.: Climate variations and the physiological basis of temperature dependent
645 biogeography: systemic to molecular hierarchy of thermal tolerance in animals, Comparative
646 Biochemistry and Physiology Part A, 739–761 pp., 2002.
647
648 Pozo Buil, M. and Di Lorenzo, E.: Decadal dynamics and predictability of oxygen and
649 subsurface tracers in the California Current System, Geophys Res Lett, 44, 4204–4213,
650 https://doi.org/10.1002/2017GL072931, 2017.
651
652 Rodgers, K. B., Lin, J., and Frölicher, T. L.: Emergence of multiple ocean ecosystem drivers in a
653 large ensemble suite with an Earth system model, Biogeosciences, 12, 3301–3320,
654 https://doi.org/10.5194/bg-12-3301-2015, 2015.
655
656 Rosewarne, P. J., Wilson, J. M., and Svendsen, J. C.: Measuring maximum and standard
657 metabolic rates using intermittent-flow respirometry: A student laboratory investigation of
658 aerobic metabolic scope and environmental hypoxia in aquatic breathers, J Fish Biol, 88, 265–
659 283, https://doi.org/10.1111/jfb.12795, 2016.
660
661 Schlunegger, S., Rodgers, K. B., Sarmiento, J. L., Frölicher, T. L., Dunne, J. P., Ishii, M., and
662 Slater, R.: Emergence of anthropogenic signals in the ocean carbon cycle, Nat Clim Chang, 9,
663 719–725, https://doi.org/10.1038/s41558-019-0553-2, 2019.
664
665 Schmidtko, S., Stramma, L., and Visbeck, M.: Decline in global oceanic oxygen content during
666 the past five decades, Nature, 542, 335–339, https://doi.org/10.1038/nature21399, 2017.
667 Smith, R., Jones, P., Briegleb, B., Bryan, F., Danabasoglu, G., Dennis, J., Dukowicz, J., Eden,
668 C., Fox-Kemper, B., Gent, P., Hecht, M., Jayne, S., Jochum, M., Large, W., Lindsay, K.,
669 Maltrud, M., Norton, N., Peacock, S., Vertenstein, M., and Yeager, S.: The Parallel Ocean
670 Program (POP) Reference Manual Ocean Component of the Community Climate System Model
671 (CCSM) and Community Earth System Model (CESM) 1, 2010.
672
673 Storch, D., Menzel, L., Frickenhaus, S., and Pörtner, H. O.: Climate sensitivity across marine
674 domains of life: Limits to evolutionary adaptation shape species interactions, Glob Chang Biol,
675 20, 3059–3067, https://doi.org/10.1111/gcb.12645, 2014.
676

https://doi.org/10.5194/egusphere-2023-2822
Preprint. Discussion started: 4 December 2023

677 Tiano, L., Garcia-Robledo, E., Dalsgaard, T., Devol, A. H., Ward, B. B., Ulloa, O., Canfield, D.
678 E., and Peter Revsbech, N.: Oxygen distribution and aerobic respiration in the north and south
679 eastern tropical Pacific oxygen minimum zones, Deep Sea Res 1 Oceanogr Res Pap, 94, 173–
680 183, https://doi.org/10.1016/j.dsr.2014.10.001, 2014.
681
682 Vaquer-Sunyer, R. and Duarte, C. M.: Thresholds of hypoxia for marine biodiversity, 2008.
683
684